

## **Radiolysis of proteins in the solid state: an approach by EPR and product analysis**

**Hélène Terryn, Véronique Deridder, Cécile Sicard-Roselli, Bernard Tilquin and Chantal Houée-Levin**

Copyright © International Union of Crystallography

Author(s) of this paper may load this reprint on their own web site provided that this cover page is retained. Republication of this article or its storage in electronic databases or the like is not permitted without prior permission in writing from the IUCr.

## Radiolysis of proteins in the solid state: an approach by EPR and product analysis

Hélène Terryn,<sup>a</sup> Véronique Deridder,<sup>a</sup> Cécile Sicard-Roselli,<sup>b</sup> Bernard Tilquin<sup>a</sup> and Chantal Houée-Levin<sup>b\*</sup>

<sup>a</sup>Université Catholique de Louvain, Faculté de Médecine, Département de Pharmacie, Unité CHAM 72.30, 72 Av. E. Mounier, B-1200 Bruxelles, Belgium, and <sup>b</sup>Laboratoire de Chimie Physique, UMR 8000 CNRS-Université Paris XI, Centre Universitaire, F-91405 Orsay CEDEX, France.  
E-mail: chantal.houee@lcp.u-psud.fr

Radio-induced modifications in proteins have been studied using several techniques. Electron paramagnetic resonance (EPR) was used to characterize free radicals, and analysis methods (high-performance liquid chromatography, capillary electrophoresis) were employed to visualize final degraded forms. Whereas EPR indicates that perthiyl radicals are formed, analysis does not detect any compound in which such bonds would be broken. Since EPR signals decay with time, it is concluded that rearrangements occur at subsequent steps, in which the solvent used during the analysis might play a role.

**Keywords:** protein radiolysis;  $\gamma$ -irradiation; high-energy electron irradiation; EPR; sulfur free radicals; radiosterilization.

### 1. Introduction

Many studies have been devoted to protein radiolysis in the solid state, mostly because of the necessity to improve protocols of sterilization of drugs and food. Also, the radiation inactivation method is still used to estimate the molecular size of membrane-bound enzymes, receptors and transport systems *in situ* (for review, see Kempner, 1999). Recently, it has been observed that irradiating cryocooled (100 K) protein crystals with synchrotron X-radiation in order to obtain crystallographic data results in radiation damage to the proteins, which alters the quality of the data. In this latter case it should be noted that the doses are extremely high ( $\sim 10^7$  Gy), *i.e.* 1000 times more than in  $\gamma$ -radiation chemistry studies. The properties of the ionizing radiation are also very different: the linear energy transfer (LET) of  $\gamma$ -rays from <sup>60</sup>Co is very low ( $0.2 \text{ keV } \mu\text{m}^{-1}$ ), but that of X-rays is very high ( $\sim 6 \text{ keV } \mu\text{m}^{-1}$ ). However, it appears that crystallography can be used as a powerful tool to investigate radiation damage to proteins at the free-radical level (Weik *et al.*, 2000).

In both radiosterilization and crystallography it is necessary to improve radioprotection, which means understanding the basic events that happen in the solid state. The existing knowledge of solid-state irradiation processes is much less than in liquid aqueous solutions, because we do not have an efficient tool such as pulse radiolysis that allows the characterization of free radicals by their absorption spectra and enables the rate constants to be measured. In the solid state the main ways of investigation are EPR spectroscopy, product analysis and, now, careful examination of damage observed in crystallographic studies. Hence the primary physicochemical

events, such as the involvement of direct *versus* indirect effects, are not understood and we can only hypothesize about the eventual rearrangements, energy migration and the roles of the solvent and of the irradiation atmosphere.

#### 1.1. Final degraded forms

It is known that irradiation of proteins in frozen aqueous solutions (193 K) as well as in lyophilized powder leads to fragmentation [for review see, for example, Houée-Levin & Sicard-Roselli (2001), and references therein]. Fragmentation does not occur randomly (Karlish & Kempner, 1984; Solomonson *et al.*, 1987; Le Maire *et al.*, 1990; Potier *et al.*, 1994; Filali-Mouhim *et al.*, 1997). In frozen aqueous solutions, fragmentation appears as a surface phenomenon (Audette *et al.*, 2000) mostly in solvent-exposed loops, indicating a role of the solvent. Amino acids with acidic or amide residues are often involved (Filali-Mouhim *et al.*, 1997).

In synchrotron X-ray experiments, observations on cryocooled protein crystals are somewhat different. One observes breakages of disulfide bonds, decarboxylation of aspartate and glutamate residues, a loss of hydroxyl groups from tyrosine and of the methylthio group of methionine, but apparently no breakage of the peptidic bond (Burmeister, 2000; Ravelli & McSweeney, 2000; Weik *et al.*, 2000).

In all types of experiments the susceptibility to radiation damage of residues of the same kind varies within the protein, and the reasons for these variations are not totally understood.

Thus damage at the free-radical level is different from that detected by chemical analysis.

### 1.2. Effect of temperature

All investigations lead to the conclusion that radio-sensitivity increases with irradiation temperature (Garman, 2003). For free-radical stability, information comes mostly from studies of the dosimeter alanine. The electron paramagnetic resonance (EPR) spectra of alanine powder irradiated at room temperature are dominated by the well known room-temperature-stable alanine radical  $\text{CH}_3\text{C}^\bullet\text{HCOOH}$ . Upon heating of room-temperature-irradiated alanine powder, a strong decay of the signal is observed, and the features of the spectrum which have recently been ascribed to a second stable radical in alanine irradiated at room temperature become more pronounced, providing an experimental isolation of this second alanine radical (Vanhaelewyn *et al.*, 1999).

In ox liver catalase, a tetrameric enzyme in solution, Potier *et al.* (1994) suggested that the radiolytic inactivation of oligomers is a two-step mechanism involving (i) fragmentation of the hit monomer, followed by (ii) temperature-dependent energy transfer from the fragmented monomer towards the associated protomer.

### 1.3. Effect of scavengers

It seems that scavengers do protect proteins during irradiation, indicating that, even at very low temperature, indirect effects would be predominant. Electron scavengers seem more efficient than  $\text{OH}^\bullet$  scavengers in frozen aqueous solutions at 193 K (Audette *et al.*, 2005), in agreement with the higher diffusion constant of trapped electrons than of  $\text{OH}^\bullet$  in solids. However,  $\text{OH}^\bullet$  scavengers seem efficient at very high concentration as has been observed in crystallographic studies (Murray & Garman, 2002).

### 1.4. Effect of dose and radiation quality

Many studies have been devoted to the alanine dosimeter and the ratio of peaks observed by EPR as a function of the dose and the LET (Malinen *et al.*, 2002, 2003). It appears that neither the dose (between 6 Gy and 60 kGy) nor the photon energy (from 10 keV to 15 MeV) affect this ratio.

In this work our aim was to identify the effect of the irradiation atmosphere. We selected two approaches, EPR and product analysis. EPR was used to detect free radicals in insulin powder. Insulin is a polypeptide hormone that contains 51 amino acids ( $M = 5808$  Da). It is made of two polypeptidic chains: chain A (21 amino acids) and chain B (30 amino acids). The two chains are linked by two disulphide bonds (A7–B7 and A20–B19). There is also an intrachain disulfide bond in chain A (A6–A11). For final product analysis, we chose hen egg-white lysozyme. It is a member of the *c*-type lysozyme family. It is made of one chain of 129 amino acids. We chose this protein for the following reasons: (i) EPR spectra from irradiated lysozyme solid are similar to those of insulin spectra reported in this paper, and (ii) it is possible to use electrophoresis methods and to check enzymatic activity, which provides powerful markers of the final fate of the free radicals. Many studies have been carried out on lysozyme, mostly in

liquid or frozen aqueous solution (Filali-Mouhim *et al.*, 1997; Bergès *et al.*, 1997; El Hanine Lmoumene *et al.*, 1999, 2000; Audette *et al.*, 2000). It has four disulfide bonds whose free-radical reactivity is known in aqueous solution and in the solid state (Bergès *et al.*, 1997; El Hanine Lmoumene *et al.*, 1999, 2000; Audette *et al.*, 2000; Weik *et al.*, 2000).

## 2. Materials and methods

### 2.1. Materials

Insulin was purchased from Novo Nordisk Pharma (insulin, Human recombinant, humidity 9.2%). It was stored in the dark at 253 K. Hen egg-white lysozyme was from Sigma and was used as received (level of hydration 9%). Acetonitrile was from Carlo Erba Reagenti. The other chemicals were purchased from Prolabo and were of the highest grade available. Water was purified using Elga Maxima system (resistivity 18.2 m $\Omega$ ).

### 2.2. Irradiations

Insulin samples were irradiated in sealed glass vials protected from light and then put into Eikosha (Japan) ESR spectrosil tubes (outer diameter 4.7 mm and inner diameter 3.8 mm) which were filled to reach a height of 6 cm.  $\gamma$ -Rays came from a panoramic  $^{60}\text{Co}$  chamber (UCL, Louvain-La-Neuve, Belgium). This source was calibrated by alanine dosimetry: alanine pellets were supplied and analyzed by Risø National Laboratory (Denmark). The determined dose rate was 350 Gy h $^{-1}$  in April 2003.

The electron beam facility used was a double-beam linear electron accelerator (LINAC) (Mönlycke, Waremmé, Belgium). The beam power of each electron generator is 20 kW. The accelerated electrons were delivered in pulses of 474 and 478 Hz. The dose rate of the double LINAC is  $\sim 10^6$  Gy min $^{-1}$ . An internal standard, a polymethylmethacrylate (PMMA) film, was used to control the delivered dose. In both cases the dose was equal to 10 kGy.

For the study at room temperature the solids were irradiated with  $\gamma$ -rays or with an electron beam, in air or under vacuum. In this case insulin samples were deoxygenated using a vacuum line. For the study of evolution of spectra *versus* time, all samples were stored at 253 K afterwards in air. For the low-temperature study, the solids were irradiated by  $\gamma$ -rays at 193 K (dry ice) or at 77 K (liquid nitrogen) in air.

For hen egg-white lysozyme, irradiations took place in a  $^{60}\text{Co}$  panoramic irradiator (IL60PL Cis-Bio International). The dose rate was equal to 3500 Gy h $^{-1}$  (verified by Fricke's dosimetry). The protein was irradiated as a solid under different atmospheres (air, nitrogen or oxygen). Gases were provided by Air Liquide (France). The protein was put under a flow of the chosen gas in dim light for 1 h before irradiation to avoid eventual photolysis.

After irradiation, the protein was re-suspended in a 20 mM phosphate buffer (Prolabo PA) pH 7 solution to a final concentration of 1 mg ml $^{-1}$ .

# radiation damage

## 2.3. EPR measurements

All EPR spectra were recorded with a Bruker EMX X-band (9.3 GHz) spectrometer. The spectrometer operating conditions adopted during the experiment were as follows: microwave power 1.008 mW for all quantitative measurements and from 0.02 to 20 mW for power saturation studies; modulation frequency 100 kHz; time constant 40.96 ms; conversion time 40.96 ms; resolution 1024; central width 332 mT; sweep width 30 mT; modulation amplitude 0.1 mT (DPPH) or 0.3 mT (insulin); receiver gain  $1 \times 10^3$  (DPPH) or  $1 \times 10^4$  (insulin); the temperature was room temperature (room-temperature study) or 77 K (very low temperature study) or from 173 to 298 K (low-temperature study). For the latter study, the temperature of the samples was first increased to 298 K starting from 173 K with increments of 25 K, and finally was decreased again to 173 K. Five scans were recorded.

The absolute  $g$ -values were determined by comparison with a Bruker reference [1,1-diphenyl-2-picrylhydrazyl (DPPH) powder sample ( $g = 2.0036$ )]. Data were treated using Bruker WinEPR. Double integration (DI) and normalized double integration (DI/N) were given by the Bruker WinEPR software. DPPH was also used to verify the day-to-day response of the spectrometer by measuring DI/N.

## 2.4. Electrophoresis

Capillary electrophoresis analyses were performed on a Beckman P/Ace 5000 system. A fused silica capillary of 75  $\mu\text{m}$  internal diameter and 57 cm length was used. Experimental conditions were: detection 214 nm; voltage 8 kV; injection time 5 s; temperature 296 K.

The electrolyte used was made with 60 mM phytic acid dodecasodium salt (Sigma) with a final pH of 9.5 made by adding phosphoric acid (Prolabo).

SDS PAGE electrophoresis was performed using 12% acrylamide-bisacrylamide gel in tris-tricine buffer pH 8.5. Reductive conditions were obtained by adding  $\beta$ -mercaptoethanol (to reduce disulfide bonds) to the sample solution to a final concentration of 20  $\mu\text{l ml}^{-1}$ .

## 2.5. High-performance liquid chromatography

High-performance liquid chromatography was performed on a Beckman Gold 168 (Beckman Coulter) instrument with diode array detection. The analytical column was a C18 reverse-phase column (3  $\mu\text{m}$ , 100  $\text{\AA}$ , 100 mm  $\times$  2.1 mm). The mobile phase eluents were: A = 0.1% trifluoroacetic acid in water and B = 0.1% trifluoroacetic acid and 70% acetonitrile in water. The protein solution was injected after dilution in an equal volume of eluent B and the gradient used was 40–100% of B in 30 min with a flow of 0.2  $\text{ml min}^{-1}$ .

## 2.6. Activity measurements

Lysozyme activity measurements were made based on the decrease in absorbance of a solution of *Micrococcus lysodeikticus* at 405 nm (Jolles *et al.*, 1965). The concentration of *Micrococcus lysodeikticus* was 1  $\text{mg ml}^{-1}$  in 10 mM phosphate

buffer pH 6.2. The measure was started just after addition of 10  $\mu\text{l}$  of a 0.1  $\text{mg ml}^{-1}$  solution of lysozyme in the same buffer.

## 3. Results

### 3.1. Free radicals in insulin

**3.1.1. Room-temperature study.** Human insulin was irradiated with 10 kGy (unless otherwise stated)  $\gamma$ -rays or by an electron beam (e-beam). The major difference between  $\gamma$  and e-beam irradiation is the dose rate: it is far lower for  $\gamma$ -rays. The irradiation time is a few seconds for e-beam exposure in comparison with 28 h for  $\gamma$ -rays. The sample was either in an air atmosphere or in vacuum for e-beam and for  $\gamma$ -rays. Both the irradiation and the recording of the spectra were performed at room temperature. Unirradiated human insulin exhibits no EPR signal.

A very simple EPR spectrum consisting of one line appearing at a  $g$  value of 2.0047 is recorded (Fig. 1a) in  $\gamma$ -irradiated human insulin in an air atmosphere. The signal is 7.5 mT broad and has no fine structure. However, several radicals may be present.

The spectrum of human insulin irradiated by  $\gamma$ -rays under vacuum is shown in Fig. 1(b). The signal here is wider (15 mT) and new lines appear.

Some high  $g_z$  values are characteristic.  $g$ -Values ( $g = 2.056$ , 2.029, 2.024) match those proposed for the perthiyl radical (RSS $\cdot$ ). A typical R-CH $_2$ -S-S $\cdot$  radical exhibits an EPR spectrum with a rhombic  $g$ -tensor ( $g_z = 2.056$ ,  $g_y = 2.025$  and  $g_x = 2.002$ ) (Becker *et al.*, 1988; Lassmann *et al.*, 2003; Engalytcheff *et al.*, 2004). The low-field component  $g_z$  is visible and characteristic but  $g_x$  is hidden in the high-field part of the spectrum and  $g_y$  is slightly modified by the presence of another radical ( $g = 2.029$  is the value registered here at the peak of the line

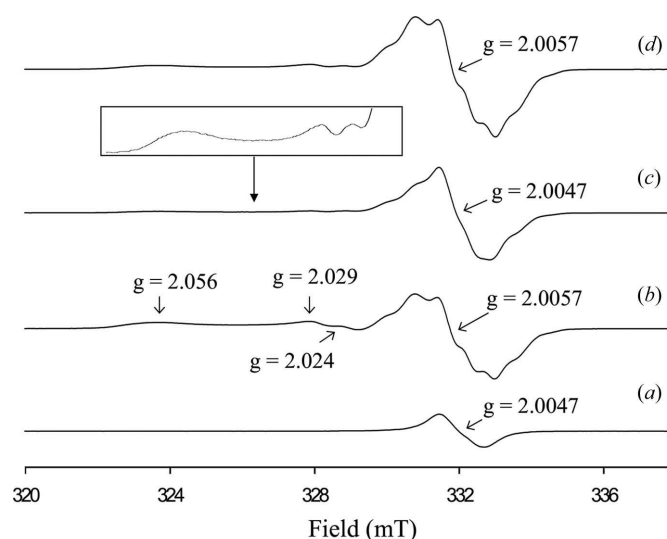


**Figure 1** EPR spectra of human insulin irradiated under different conditions at room temperature: (a)  $\gamma$ -irradiated human insulin in air; (b) irradiated by  $\gamma$ -rays under vacuum; (c) irradiated by electron beam in air; (d) irradiated by electron beam under vacuum.

for the perthiyl radical). Similar spectra were reported for hen egg-white lysozymes (A. Faucitano, personal communication).

The spectrum of human insulin irradiated by the e-beam in the presence of air (Fig. 1c) is more complex than that for  $\gamma$ -irradiation shown in Fig. 1(a). The signal attributed to the perthiyl radical is present. Conversely, the spectra recorded in vacuum without oxygen shown in Figs. 1(d) (e-beam) and 1(b) ( $\gamma$ -rays) are very similar [same  $g$ -values, same DI/N (normalized double integration), *i.e.* same quantities of unpaired electrons, same complex process of microwave saturation].

The study of the power saturation of each line provides information on the identities of the radicals. These amplitudes vary as a function of the square root of the microwave power. They all increase and reach a steady state. The power at which the steady state occurs depends on the radical. Perthiyl radicals, C-centred radicals and thiyl radicals exhibit different saturation behaviours (Lassmann *et al.*, 2003; Gibella *et al.*, 2000).

The intensity of the line for  $\gamma$ -irradiated insulin in air saturates at a low microwave power (8 mW). The  $g$ -value (2.0047) and the low-power saturation indicate carbon-centred radicals.

Fig. 2 shows the saturation curves of the different peaks of  $\gamma$ -irradiated human insulin under vacuum. Two different trends emerge from the graphic. Peaks 1, 2 and 3 keep increasing in proportion to the square root of the microwave power. Together with the  $g$ -values, this observation is in agreement with the hypothesis that sulfur-centred radicals are present, that saturate at high power. Conversely, peaks 4, 5, 6

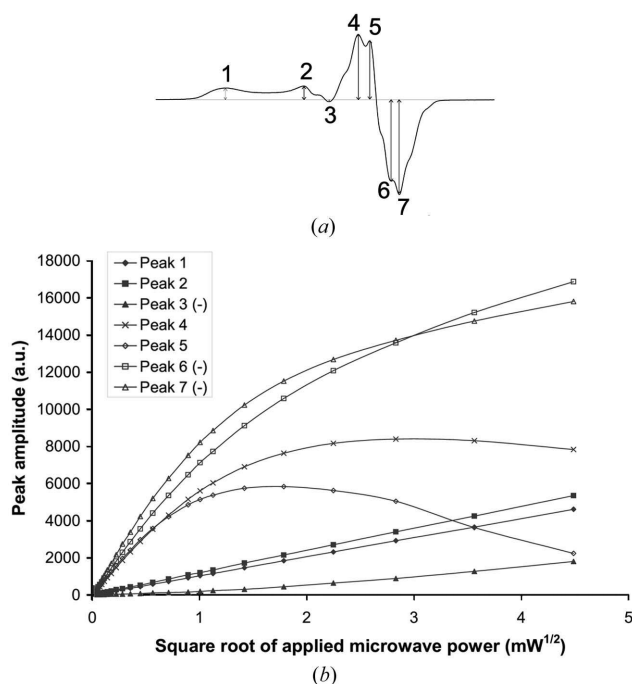


**Figure 2** Effect of the microwave power on the individual peaks of the human insulin spectrum. Spectrum of  $\gamma$ -irradiated human insulin under vacuum and numeration of the seven different peaks (a), and the amplitude of each peak as a function of the square root of the microwave power (b).

and 7 saturate at different lower powers, as would be expected for signals from several carbon-centred radicals. In addition, EPR spectra of carbon-centred radicals are relatively more intense at low microwave power (Lassmann *et al.*, 2003).

A similar study was carried out for e-beam-irradiated insulin with and without oxygen at room temperature. The same trends were observed (not shown), which lead to the same conclusions.

Fig. 3 shows the evolution of EPR spectra of human insulin irradiated by an electron beam under vacuum. The same results as above are observed under different conditions. All spectra tend to evolve towards the simple signal of  $\gamma$ -irradiated insulin in air (Fig. 1a)

The peaks attributed to a perthiyl radical and to some carbon-centred radicals decrease without the appearance of other signals. A slow radical decay (50–70% of DI/N over a period of 140 days) is observed in air.

The determination of the quantities of free radicals was performed using the DI/N of the first-derivative spectrum, given by the Bruker WinEPR software. To ensure that power saturation did not occur, a microwave power of 1.008 mW was predetermined as the level where this unwanted effect did not occur. The predetermination involved selecting a power in the linear region of the plot of the square root of microwave power against peak intensity. Fig. 4 shows that DI/N increases linearly with the dose (irradiation in air atmosphere).

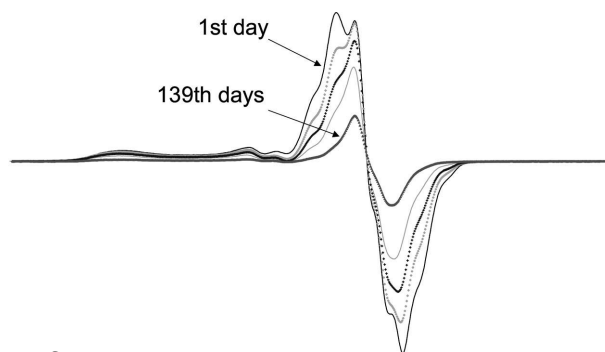


**Figure 3** EPR spectra versus elapsed time [days from 1 (top) to 139 with 13, 29 and 70 days as intermediates] for human insulin irradiated by electron beam under vacuum.

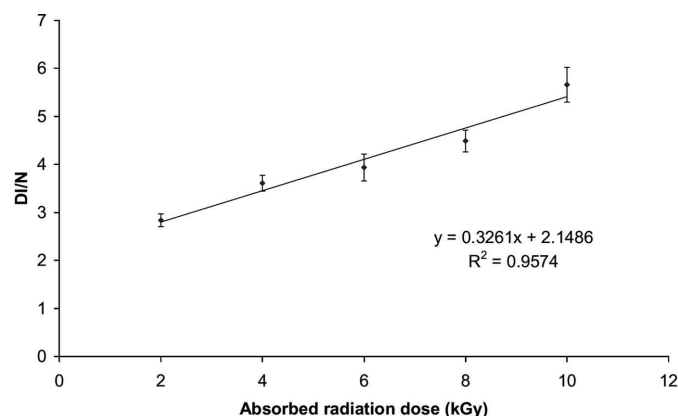


**Figure 4** DI/N (double integration normalized in arbitrary units) of EPR spectra of  $\gamma$ -irradiated human insulin in air versus the absorbed radiation dose.

## radiation damage

At constant dose, DI/N of  $\gamma$ -irradiated insulin in vacuum is about 14 times higher than in air. Dose rate also has an effect: DI/N of e-beam-irradiated insulin in air is about seven times higher than that of  $\gamma$ -irradiated insulin in the same atmosphere.

The radiolytic radicals yield was determined through comparison of the EPR signals areas with that of alanine standards measured under similar experimental conditions (EPR parameters, temperature). The laboratory calibration curve (Engalytcheff *et al.*, 2003) was taken to determine radical yield. The radical yield of  $\gamma$ -irradiated insulin in air for a dose of 10 kGy is  $4.5 (\pm 0.18) \times 10^{-9}$  mole  $J^{-1}$  (mean of five assays).

**3.1.2. Influence of the temperature.** Temperature does not affect the primary steps of radiolysis. The quantity of trapped radiation products at low temperature should not differ from that at room temperature in the limit of uncertainty (Miyazaki *et al.*, 1994). However, some subsequent steps, such as the diffusion of oxygen, are temperature-dependent.

Human insulin was irradiated by  $\gamma$ -rays in air at very low temperature (77 K in liquid nitrogen) and the spectrum was recorded at the same temperature without warming the sample (Fig. 5). A  $g_z$  value in agreement with the formation of a peroxy radical ( $g_z = 2.037$ ) is visible although it is very close to the  $g_z$  value of perthiyl radical. Peroxy radicals have been characterized previously ( $g_z = 2.035$ ,  $g_y = 2.008$ ,  $g_x = 2.002$ ) (Sevilla *et al.*, 1988; Swarts *et al.*, 1989). This line (2.037) also appears at 173 K (Fig. 6)

To study the effect of warming on the EPR spectra, the samples were irradiated at 193 K (in dry ice). The first spectrum was recorded at 173 K. The temperature of the samples was then increased to room temperature (298 K) starting from 173 K with an increment of 25 K, and EPR spectra were recorded at each temperature. Finally the temperature was decreased again to 173 K and the spectrum recorded again. The results are given in Fig. 6.

EPR spectra of  $\gamma$ -irradiated insulin in air at low temperature show the same lines as those under vacuum at room temperature. The perthiyl radical is present and there is no longer evidence of peroxy radicals. Upon increasing the temperature, the intensity of the peaks reduces unequally. For instance, peak 4 (see Fig. 2 for the numbering) decreases more than peak 5. As a consequence, the spectrum appears more structured. Upon cooling again, the intensity is not restored. Observed changes when temperature increases are thus irreversible, indicating that the loss of intensity is due to free-radical recombination and/or to reaction with oxygen. After 16 days of storage at 253 K, the measured spectrum is like that obtained from irradiating the sample at room temperature (Fig. 1a).

### 3.2. Lysozyme: final products

Similar spectra of sulfur free radicals have been observed following the  $\gamma$ -irradiation of hen egg-white lysozyme (A.

**Table 1**

Initial yields of disappearance of hen egg-white lysozyme after irradiation under different atmospheres.

	Electrophoresis (mol $J^{-1}$ )		
	Under $O_2$	Under $N_2$	Under air
Lysozyme peak decrease measured using capillary	$3.2 (\pm 0.4) \times 10^{-10}$	$2.4 (\pm 0.3) \times 10^{-10}$	$3.4 (\pm 0.4) \times 10^{-10}$

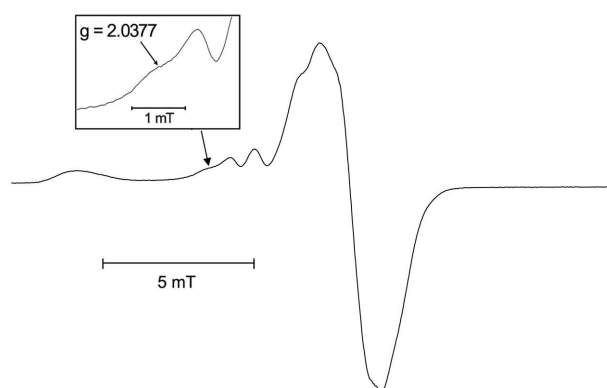


**Figure 5**

EPR spectrum of human insulin irradiated by  $\gamma$ -rays in air at 77 K recorded at the same temperature.

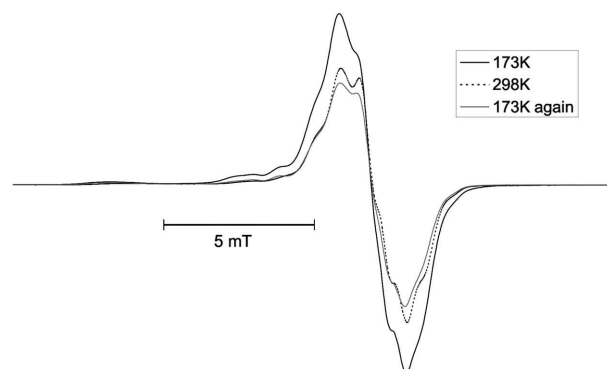


**Figure 6**

EPR spectra of human insulin irradiated by  $\gamma$ -rays in air at 198 K recorded at different temperature.

Faucitano, personal communication). To date, no final degradation form of this protein involved sulfur functions. Thus the second approach of this study was to quantify the degradation products of hen egg-white lysozyme after  $\gamma$ -irradiation from 0 to 20 kGy in the solid state (lyophilized powder), to formulate a hypothesis about the fate of the free-radical site initially located on sulfur.

Irradiation of lyophilized powders was performed at room temperature under three different atmospheres (air, nitrogen and oxygen) to gain insights into the reactions of oxygen with free radicals and their influence on the nature of final compounds.

According to capillary electrophoresis, three degradation products are formed after irradiation with one peak dominant whatever the gas used. The dependence of product formation over the dose was calculated and the disappearance yield of the lysozyme peak is summarized in Table 1. Chromatograms

of irradiated lysozyme also exhibit three new peaks, one of them being predominant as for capillary electrophoresis. Comparison between the three atmospheres studied shows that the same degradation products are formed, although the concentration of these products seems lower when nitrogen is used (Table 1). These yields are one order of magnitude lower than that of free radicals in insulin.

Electrophoresis gels (SDS PAGE) of lysozyme were performed under reductive or non-reductive conditions (not shown). Under O<sub>2</sub> or air, no new band corresponding to an aggregation or to fragmentation was observed, indicating that  $\gamma$ -irradiation did not induce a backbone fragmentation detectable with SDS PAGE in this dose range. Indeed, all reported fragmentations took place at higher doses [ $\sim$ 60 kGy or higher (Filali-Mouhim *et al.*, 1997)]. Conversely, the same experiments performed on  $\alpha$ -lactalbumin in the same dose range lead to aggregation products (C. Sicard-Roselli, unpublished).

Enzymatic activity decreases weakly upon increasing the dose (25% for 10 kGy). One can conclude that the disulfide functions that are essential for the enzymatic activity (all except the 6–127 bond) do not seem affected. However, the 6–127 bond, which is also the most sensitive in aqueous solution (Bergès *et al.*, 1997), might be broken without affecting the SDS PAGE profile and the activity.

#### 4. Discussion

The aim of this work is to detect free radicals created in irradiated proteins in the solid state by EPR and to make attempts to correlate these free radicals with the final degradations.

Both proteins, insulin and lysozyme, contain only disulfide and thioether groups, and no thiol function. At the free-radical level, we notice mostly that irradiation creates sulfur and carbon-centred radicals. Whereas the carbon-centred ones are of several origins and lead to EPR signals which are difficult to assign, all sulfur radicals observed seem to have similar structures: EPR characteristics indicate RSS<sup>•</sup> perthiyl radicals, in agreement with the proposition of Hadley & Gordy (1975). In crystallography measurements, it seems that one sees mostly disulfide radical anions, *i.e.* the C–S bond does not appear broken. Disulfides have a positive electron affinity (Carles *et al.*, 2001) and are sites of electron localization giving disulfide anions (Bergès *et al.*, 2000; Houée-Levin, 2002). Theoretical studies show that the weakest bond is S–S (Pshezhetskii *et al.*, 1974; Bergès *et al.*, 2000) although in some conformations the excess electron can be localized on carbon (Bergès *et al.*, 1997). It is possible that perthiyl radicals represent some other conformation of disulfide radicals.

According to SDS PAGE, there is no fragment close to a disulfide among the final products. This might indicate that the C–S bond is restored, since the time after irradiation affects EPR spectra and there is a decay of radicals *versus* time (half life is about one month in the solid state when stored at 253 K). This decay may be a sign of electron migration to locations other than sulfur functions. However, EPR is much

more sensitive than other techniques of analysis, and the fragmentation products could represent only a few percent of the initial protein mass.

In the presence of oxygen, sulfur–oxygen radicals may be created. Their EPR characteristics are well documented. Sulfinyl radicals (R–CH<sub>2</sub>–S<sup>•</sup>=O) in proteins exhibit  $g_z = 2.021$ ,  $g_x = 2.0094$ ,  $g_y = 2.0018$  (Reddy *et al.*, 1998; Adrait *et al.*, 2002). The  $g$  values of the thiyl peroxy radical (R–S–OO<sup>•</sup>) are  $g_z = 2.035$ ,  $g_x = 2.008$ ,  $g_y = 2.002$  (Sevilla *et al.*, 1988; Swarts *et al.*, 1989); however, this radical is unstable at room temperature. Sulfonyl radicals (R–<sup>•</sup>SO<sub>2</sub>) exhibit a very small  $g$ -anisotropy ( $g = 2.0055$ ) (Becker *et al.*, 1988; Sevilla *et al.*, 1990). These values are different from ours. In addition, in our case, sulfur-centred free radicals are much more abundant in a de-aerated atmosphere. This is in favour of non-oxygenated sulfur radicals.

The dose rate and the irradiation atmosphere affect EPR spectra. Whatever the atmosphere, EPR spectra are more complex after e-beam irradiation (Fig. 1), indicating an effect of the dose rate at the free-radical level. However, at the level of final products, the difference is not so clear. The effect of the dose rate is not general: it was shown with the alanine dosimeter that intensity does not influence the shape of EPR spectra, and hence nor the kind of free radicals that are created (Malinen *et al.*, 2002). As for the quality of the radiation (LET), Malinen *et al.* (2003) have shown that the EPR spectrum of alanine is not sensitive to it. In our experiments, the LET of high-energy electrons and of  $\gamma$ -rays (1.17 and 1.20 MeV) are the same, hence the variations that we observe cannot be attributed to LET.

Sulfur-centred radicals are less abundant in the presence of air than in vacuum after high-dose-rate irradiation (e-beam), and absent after  $\gamma$ -ray irradiation. This might indicate that the free radicals decay by reaction with oxygen, since it is known that oxygen reacts with free radicals. If the dose rate is low, this reaction can take place during irradiation whereas, for very short irradiations (very high dose rate), reactions of radical with oxygen (after diffusion) are in competition with immediate radical–radical reactions during the radiolysis in the solid. However, there should be formation of some peroxy radicals. The  $g$  values for a peroxy radical (ROO<sup>•</sup>) are  $g_z = 2.035$ ,  $g_x = 2.008$  and  $g_y = 2.002$  (Engalytcheff *et al.*, 2004; Sevilla *et al.*, 1988, 1990; Swarts *et al.*, 1989). Irradiation at low temperature (77 K) allows the observation of a weak line at the  $g$  value of 2.037 but the  $g_y$  and  $g_x$  lines are mixed with lines from other radicals. At room temperature this line is no longer visible. This may explain why we do not see such radicals. As for final compounds, our results indicate that lysozyme is more radioresistant in the absence of oxygen than in its presence; however, the final products are the same. If they are formed, peroxides probably disappear by radical–radical disproportionation reactions.

We thus confirm that drastic rearrangements take place between the first free-radical step and the last final forms. If sulfur functions are the target of initial electron and/or hole localization, electron and/or hole migration takes place after irradiation. Some of the degradations may take place when the

## radiation damage

protein is put in solution. Indeed, it was shown that fragmentation sites detected for higher doses are on the protein surface in contact with the solvent (Filali-Mouhim *et al.*, 1997). As discussed above, experimental conditions are very different from cryocrystallography (dose, dose rate, LET of radiation). Other main differences exist: in crystallography, proteins are in a crystalline state whereas in our studies they are in an amorphous or microcrystalline state; for EPR, only the hydration water is present (~9%) whereas, for crystallography, crystallization buffer and glycols are present. To compare with cryocrystallography it would be interesting to test these parameters.

We would like to thank the Institut Interfacultaire des Sciences Nucléaires (IISN-FNRS) for financial support and also Nelson Beghein for technique help. We thank also Jean Cara for carrying out the irradiations.

### References

- Adrait, M., Oehrstroem, M., Barra, A.-L., Thelander, L. & Graeslund, A. (2002). *Biochemistry*, **41**, 6510–6516.
- Audette, M., Chen, X., Houee-Levin, C., Potier, M. & Le Maire, M. (2000). *Int. J. Radiat. Biol.* **76**, 673–681.
- Audette, M., Houee-Levin, C. & Potier, M. (2005). *Radiat. Phys. Chem.* **72**, 301–306.
- Becker, D., Swarts, S., Champagne, M. & Sevilla, M. D. (1988). *Int. J. Radiat. Biol.* **53**, 767–786.
- Bergès, J., Fuster, F., Jacquot, J.-P., Silvi, B. & Houée-Levin, C. (2000). *Nukleonika*, **45**, 23–30.
- Bergès, J., Kassab, E., Conte, D., Adjadj, E. & Houée-Levin, C. (1997). *J. Phys. Chem.* **101**, 7809–7817.
- Burmeister, W. P. (2000). *Acta Cryst.* **D56**, 328–341.
- Carles, S., Lecomte, F., Schermann, J. P., Desfrancois, C., Xu, S., Nilles, J. M., Bowen, K. H., Bergès, J. & Houée-Levin, C. (2001). *J. Phys. Chem. A*, **105**, 5522–5526.
- El Hanine Lmoumène, C., Conte, D., Jacquot, J.-P. & Houée-Levin, C. (1999). *Res. Chem. Intermed.* **25**, 313–321.
- El Hanine Lmoumène, C., Conte, D., Jacquot, J.-P. & Houée-Levin, C. (2000). *Biochemistry*, **39**, 9295–9301.
- Engalytcheff, A., Debuyst, R., Vanhaelewyn, G. C. A. M., Callens, F. J. & Tilquin, B. (2004). *Radiat. Res.* **162**, 616–622.
- Engalytcheff, A., Deridder, V., Debuyst, R. & Tilquin, B. (2003). *Radiat. Res.* **160**, 103–109.
- Filali-Mouhim, A., Audette, M., St-Louis, M., Thauvette, L., Denoroy, L., Penin, F., Chen, X., Rouleau, N., Le Caer, J. P., Rossier, J., Potier, M. & Le Maire, M. (1997). *Int. J. Radiat. Biol.* **72**, 63–70.
- Garman, E. (2003). *Curr. Opin. Struct. Biol.* **13**, 545–551.
- Gibella, M., Crucq, A.-S., Tilquin, B., Stocker, P., Lesgards, G. & Raffi, J. (2000). *Radiat. Phys. Chem.* **58**, 69–76.
- Hadley, J. H. & Gordy, W. Jr (1975). *Proc. Natl. Acad. Sci. USA*, **72**, 3486–3490.
- Houee-Levin, C. (2002). *Methods Enzymol.* **353**, 35–44.
- Houee-Levin, C. & Sicard-Roselli, C. (2001). *Radiation Chemistry: Present Status and Future Prospects*, edited by C. Jonah and B. M. Rao, pp. 553–584. Amsterdam: Elsevier.
- Jolles, J., Spotorno, G. & Jolles, P. (1965). *Nature (London)*, **208**, 1204–1205.
- Karlish, S. J. D. & Kempner, E. S. (1984). *Biochim. Biophys. Acta*, **776**, 288–298.
- Kempner, E. S. (1999). *Anal. Biochem.* **276**, 113–123.
- Lassmann, G., Kolberg, M., Bleifuss, G., Gräslung, A., Sjöberg, B.-M. & Lubitz, W. (2003). *Phys. Chem. Chem. Phys.* **5**, 2442–2453.
- Le Maire, M., Thauvette, L., de Foresta, B., Viel, A., Beauregard, G. & Potier, M. (1990). *Biochem. J.* **267**, 431–439.
- Malinen, E., Heydari, E. O., Hole, E. O. & Sagstuen, E. (2002). *Radiat. Res.* **158**, 23–32.
- Malinen, E., Hult, E. A., Hole, E. O. & Sagstuen, E. (2003). *Radiat. Res.* **159**, 149–153.
- Miyazaki, T., Arai, J., Kaneko, J., Yamamoto, K., Gibella, M. & Tilquin, B. (1994). *J. Pharm. Sci.* **83**, 1643–1644.
- Murray, J. & Garman, E. (2002). *J. Synchrotron Rad.* **9**, 347–354.
- Potier, M., Villemure, J. F. & Thauvette, L. (1994). *Biochem. J.* **298**, 571–574.
- Pshezhetskii, S. Y., Kotov, A. G., Milinchuk, V. K., Roginskii, V. A. & Tupikov, V. I. (1974). Editors. *EPR of Free Radicals in Radiation Chemistry*, pp. 223–286. New York: Wiley.
- Ravelli, R. B. G. & McSweeney, S. M. (2000). *Structure*, **8**, 315–328.
- Reddy, S. G., Wong, K. K., Parast, C. C., Peisach, J., Magliozzo, R. S. & Kozarich, J. W. (1998). *Biochemistry*, **37**, 558–563.
- Sevilla, M. D., Becker, D. & Yan, M. (1990). *Int. J. Radiat. Biol.* **57**, 65–81.
- Sevilla, M. D., Yan, M. & Becker, D. (1988). *Biochem. Biophys. Res. Commun.* **155**, 405–410.
- Solomonson, L. P., McCreery, M. S., Kay, C. S. & Barber, M. J. (1987). *J. Bio. Chem.* **262**, 8834–8837.
- Swarts, S., Beckers, D., DeBolt, S. & Sevilla, M. D. (1989). *J. Phys. Chem.* **93**, 155–161.
- Vanhaelewyn, G. C., Mondelaers, W. K. & Callens, F. J. (1999). *Radiat. Res.* **151**, 590–594.
- Weik, M., Ravelli, R. B., Kryger, G., McSweeney, S., Raves, M. L., Harel, M., Gros, P., Silman, I., Kroon, J. & Sussman, J. L. (2000). *Proc. Natl. Acad. Sci. USA*, **97**, 623–628.